Investigation of bearing capacity factor of T-bar penetrometer at shallow depths in clayey soils

Márcio S.S. Almeida*, José Renato M.S. Oliveira, Khader I. Rammah and Pablo C. Trejo
Graduate School of Engineering, COPPE, Federal University of Rio de Janeiro, Brazil

Abstract. The T-bar penetrometer is normally used in both *in-situ* and on the centrifuge to establish profiles of the undrained shear strength of fine-grain soils. However, adequate measurement of the undrained shear strength at shallow depths requires understanding the failure mechanism at these depths.

For onshore and offshore structures such as pipelines, the assessment of soil parameters, in particular the undrained shear strength at shallow depth can be very critical to achieve both efficient and economic design. However, this requires the evaluation of the value of T-bar bearing factor (N_b) corresponding to both shallow and very shallow depths.

This paper describes a series of geotechnical centrifuge tests undertaken using three different sizes of the T-bar penetrometer on two types of clayery soil.

The results of the undrained strength obtained from each T-bar were compared with the results obtained from the bigger T-bars. The curves that describes the variation of the T-bar factor (N_b) versus the penetration depth were established from the comparison of all results obtained from the three different sizes of the T-bar. The results of (N_b) obtained in this study were compared with results obtained from both numerical and analytic solutions proposed in the literature.

Generally, the experimental data obtained in this study presented N_b values higher than those predicted by others authors for all H/D ratios. However, the comparison indicates that the N_b values obtained in this study showed relatively reasonable agreement with those values obtained from the literature by adopting a non-homogenous strength profile.

Keywords: T-bar penetrometer, physical modelling, geotechnical centrifuge, clay, shallow depths

1. Introduction

The use of penetrometer probes in fine-grained soils to measure undrained shear strength at shallow depths requires the comprehension of how the failure mechanisms behave in intermediate situations in which the probe cannot yet be considered deeply buried [1].

That is the case of the T-bar penetrometer which has been widely used *in situ*, mainly offshore [2, 3], and also in physical modelling for the measurement of very soft clay strength profiles [4, 5]. The equation that associates force readings with the undrained shear strength is only valid for deep penetration failure mechanisms.

However, for onshore and offshore structures such as pipelines, the study of very shallow soil parameters is vital for an efficient and economic design. Most lifelines are inserted less than two diameters in the seabed soil; therefore cost-effective ways to evaluate the strength profile are much appreciated.

*Corresponding author: Márcio S.S. Almeida, Graduate School of Engineering, COPPE, Federal University of Rio de Janeiro, Caixa Postal 68506, CEP 21945-970, Brazil. Tel.: +55 21 25627200; E-mail: mssal@globo.com.

This paper describes a series of geotechnical centrifuge T-bar penetrometer tests undertaken with three different sizes on the same soil sample. The smaller probes' undrained strength results are compared with those of the larger ones, leading to a T-bar bearing factor (N_b) curve that indicates the appropriate values for very shallow depths. These data are also compared with numerical analysis and analytic equations proposed in the literature.

2. T-bar Penetrometer

The T-bar penetrometer was originally developed for use in centrifuge testing [4, 6], aimed at providing a continuous profile of the undrained strength of clay beds. It comprises a cylindrical bar that is attached perpendicularly to the penetrometer shaft and has a projected area of 5 to 10 times the shaft area. The principle of this penetrometer is to force the soil to flow around the probe, minimising the relative magnitude of the volume expansion of the soil due to the insertion of the shaft. In this way, the correction of the measured penetration resistance due to the overburden stress is minimised [7].

A number of other flow type penetrometers have been proposed [2] but the T-bar is the most widely used, particularly in centrifuge physical modelling in relation to fine-grained soils [8].

Stewart and Randolph [6] proposed the following equation to obtain S_u from T-bar measurements based on [9]:

$$S_u = \frac{F_V}{N_b D L} \tag{1}$$

where F_V is the vertical force measured during penetration; D is the pipe diameter; L is the bar length; and N_b is the T-bar bearing factor.

Alternatively, Equation (1) can be written as:

$$S_u = q_m / N_b \tag{2}$$

where q_m is the measured resistance during penetration.

Chung and Randolph [1] and Randolph [10] suggested a correction on the measured values q_m. This correction is largely dependent on the ratio between the areas of shaft (push rods) and T-bar, which is typically 0.1 to 0.2, but also depends on the total vertical stress, which is quite low in the present study. Therefore this correction is far less significant than that on the piezocone [1] and is not considered in the present paper.

The T-bar bearing factor N_b depends on the surface roughness of the bar, varying between 9.1 (fully smooth) and 11.9 (fully rough). An average value of 10.5 is recommended for general use in deep penetration conditions [10], although [11] suggested an average value of 12 based on high quality samples from ten onshore and offshore sites around the world. Low et al. [12] concluded that although theoretical solutions generally predict the trends of the field data, further studies are required to improve the theoretical solutions.

However, the T-bar factor changes at shallow embedment due to the change in bearing capacity mechanism. Barboza-Cruz and Randolph [13] investigated the penetration of a cylindrical object into soft clay, starting from a very small embedment using a large deformation finite element approach with remeshing and interpolation techniques. The results show an evolution of the bearing capacity factor for a penetration depth $H/D > 0.5\%$. Four equations are presented, considering fully smooth and fully rough interfaces and homogeneous ($S_u = 9\,kPa$) and non-homogeneous ($S_u = 5 + 1.5\,H/D$) soil profiles. Oliveira et al. [14] proposed the following polynomial adjustment (Equation 3), based on a series of numerical analysis, which is only valid for the interval $0 \leq (H/D) \leq 6$, where H is the burial depth of the bar measured from the soil surface to the lower generatrix. The soft clay soil was simulated using the Tresca model, and an interface factor $\alpha = 0.5$ was chosen to simulate an average surface roughness. A homogeneous undrained strength profile was assumed with $S_u = 1\,kPa$.

$$N_b = 0.0053 \left(\frac{H}{D}\right)^6 - 0.1102 \left(\frac{H}{D}\right)^5 + 0.9079 \left(\frac{H}{D}\right)^4 - 3.7002 \left(\frac{H}{D}\right)^3$$
$$+ 7.2509 \left(\frac{H}{D}\right)^2 - 3.9168 \left(\frac{H}{D}\right) + 5.3519 \tag{3}$$

The results indicate a mean initial value around 5.24 for $H/D = 0$, which is close to the expected Terzaghi bearing capacity factor of 5.14 for a flat plate foundation, and a mean final value around 10.5 for $H/D = 6$ which is the same proposed by [10] for a fully-buried condition.

White et al. [15] describes the interpretation of T-bar penetrometer tests at shallow depths in soft soils considering two mechanisms: soil buoyancy and the reduced bearing factor associated to shallow failure mechanism. The results show that the transition depth between shallow to deep failure behaviour vary between 2 and 8 bar diameters, for softer and stiffer soils respectively.

3. Test concept

The main objective of these tests is to evaluate the T-bar bearing factor (N_b) variation in shallow depths by comparing the strength profiles obtained with different bar sizes. The background concept is that the penetrating bar normally reaches fully-buried behaviour for depths greater than two diameters. In that way, a small T-bar with diameter D is expected to reach fully-buried behaviour at depths greater than $2D$. On the other hand, a larger T-bar with nD diameter will only reach the same condition at depths beyond $2nD$. Therefore for depths between $2D$ and $2nD$, the smaller T-bar strength profile, when compared with the larger T-bar strength profile, can be used to assess the N_b variation, provided the undrained strength values are the same at each depth (Fig. 1). Thus, the strength profile for a smaller T-bar is considered as a reference to obtain the strength profile for the bigger T-bar; this is only for depths greater than 2D. In that way, a medium T-bar can play the role of the bigger one when compared to the small one, and at the same time it can be used as a reference for the big T-bar. Equation (4) shows how the N_b factor is obtained, where index B stands for the larger T-bar and index S stands for the smaller one.

$$S_u = \frac{F_{V,B}}{N_{b,B} D_B L_B} = \frac{F_{V,S}}{N_{b,S} D_S L_S} \tag{4a}$$

$$N_{b,B} = \frac{F_{V,B}}{F_{V,S}} \frac{D_S L_S}{D_B L_B} N_b \text{ assuming that } N_{b,S} = N_b \text{ for z} > 2\text{D} \tag{4b}$$

Naturally, both $N_{b,S}$ and $N_{b,B}$ will be equal to N_b for depths greater than $2nD$.
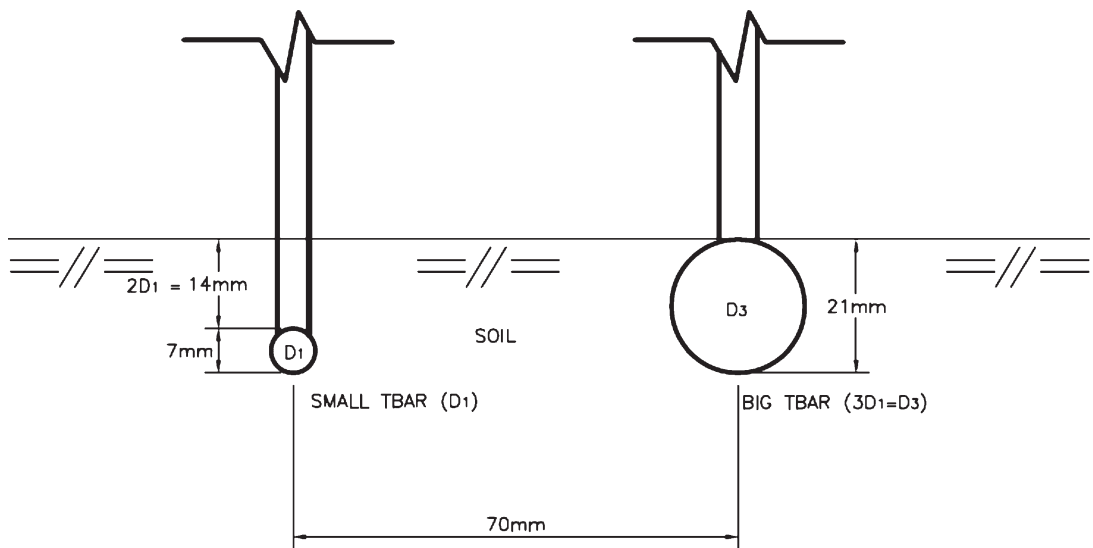
Fig. 1. Small and large T-bar test concept.

Table 1
Geotechnical properties of the kaolin-sand artificial clay mixture

Property	Value
Liquid limit, w_L	44%
Plastic limit, w_P	22%
Soil particle density, G_s	2.61
Effective unit weight, γ'	$4.7\,kN/m^3$
Coefficient of consolidation (mean value), c_v	$5.3\,m^2/yr$

Table 2
Geotechnical properties of the Roncador natural marine clay

Property	Value
Liquid limit, w_L	82%
Plastic Index, I_P	59%
Soil particle density, G_s	2.66
Effective unit weight, γ'	$6.4\,kN/m^3$
Coefficient of consolidation (mean value), c_v	$0.9\,m^2/yr$

4. Soil properties

The tests were carried out in two different soils: artificial clay made of a 75% kaolin and 25% sand mixture, and a natural marine clay from the Roncador offshore site near Rio de Janeiro [16].

The artificial clay proportion was defined based on the results of a series of shear strength and consolidation tests. The percentage that led to geotechnical parameters as close as possible to those of typical Brazilian colluvium deposits was selected. Table 1 shows the main geotechnical properties of this material.

The natural marine clay soil samples were taken from deepwater oil production sites offshore Rio de Janeiro State using a Kullenberg sampler. The material was stored in PVC tubes that were internally sealed with paraffin. The soil can be described as greyish silty clay with some sand, and is classified as high plasticity clay (CH) according to the Unified Soil Classification System. Table 2 shows the main geotechnical properties of this material.

5. Test set-up

The tests were carried out at the Alberto Luiz Coimbra Institute – Graduate School and Research in Engineering (COPPE) 1.0 m diameter 90 g-ton load capacity mini-drum geotechnical centrifuge [17]. It includes 16 data acquisition channels and a 2 step motor drive and servo-controlled actuators: a linear one and a one which turntable on which the first one is mounted. The centrifuge is capable of $90°$ movement, changing the rotation axis from the vertical to the horizontal position, allowing more complex sample preparation. COPPE's centrifuge has been mainly used in studies related to pipelines [14], penetration tests [5, 8, 16] and mudmats [18]. For the present application a strongbox of dimension 502 mm in length, 210 mm wide and 140 mm high was used.

Three miniature T-bars were developed, comprising different bar diameters of 7 mm, 14 mm and 21 mm that correspond to bar lengths of 28 mm, 56 mm and 84 mm, respectively. In such way, the medium one is twice the size of the smaller one, and the larger one is three times the size of the smaller one. The vertical force was measured using miniature tension and compression load cells, which are compensated for bending moments and thermal variations, attached to the rigid shafts that hold the bars (Fig. 2). Although the location of the load cell incorporate some contribution of the shaft friction forces during the penetration, this input was considered negligible, once the focus of the paper is the behaviour at shallow depths.

The penetration rate was adjusted according to the bar dimensions in order to keep a constant normalised velocity, which is defined as the product of the penetration velocity by the bar diameter divided by the coefficient of consolidation [19]. Therefore the small T-bar was driven at 0.3 mm/s, the medium one at 0.2 mm/s, and the larger one at 0.1 mm/s.
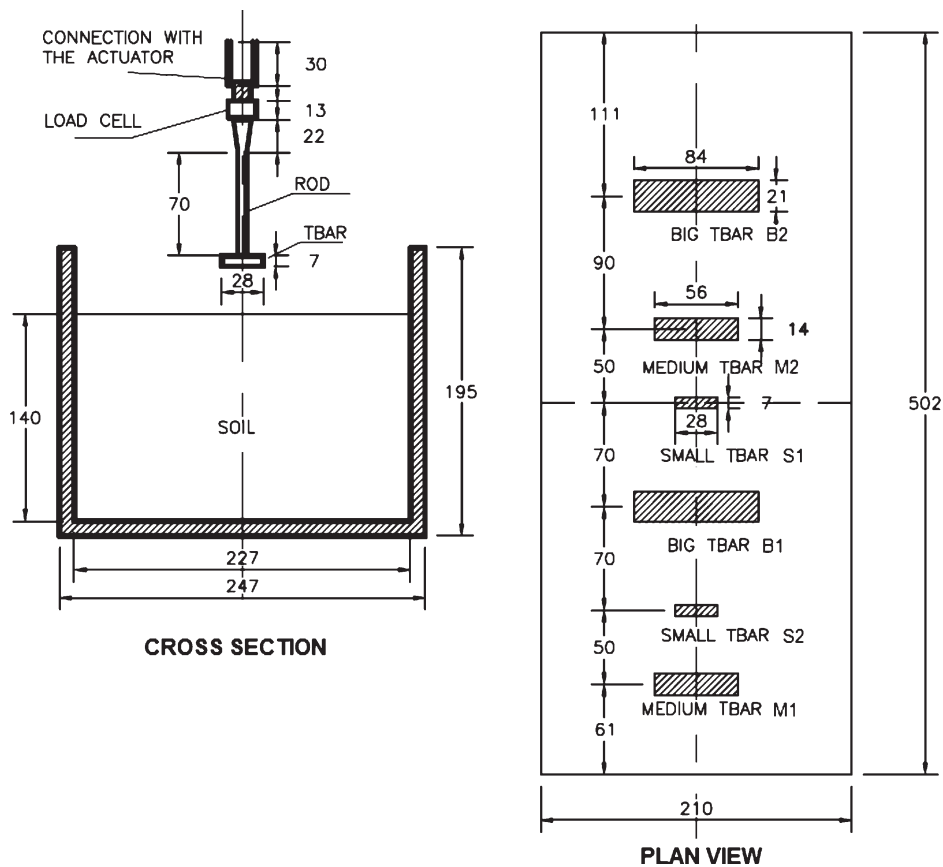
Fig. 2. Centrifuge test set-up.

A total of five tests were carried out in this study: three using the kaolin-sand clay and two using the Roncador clay. In each test, six T-bar penetration tests were undertaken: two with the small bar (S1 and S2), two with the medium bar (M1 and M2) and two with the large bar (B1 and B2). Table 3 summarises the main conditions of the tests. The penetration sequence was planned to minimize interference between tests. In that way, the bigger T-bars were performed near the smaller ones, always assuring a minimum spacing of 3.5 diameters of the bigger T-bar.

6. Sample preparation

Samples 4, 5 and 6 with the kaolin-sand mixture were divided into two phases: consolidation followed by vertical actuation both at 50 g. The sample was previously mixed in an industrial mixing machine at an initial water content of 44% which equals to the liquid limit. Afterwards, the soil was placed in the sample box using the clay lumps technique. This material was allowed to spin at 50 g over a period of 3 hours, assuring the collapse of the macro voids between the clay lumps and resulting in a nearly fully-consolidated clay layer.

Samples 9 and 10 with the Roncador clay were also divided into two phases: consolidation at 100 g followed by vertical actuation, both at 50 g. The sample was previously mixed at an initial water content of 84% (i.e., that is slightly above the liquid limit mentioned in Table 2) before being placed in the strong box, also using the clay lumps technique. This soil was allowed to consolidate at 100 g, over a period of 18 hours, again resulting in a nearly fully-consolidated clay layer. Afterwards, the acceleration level was reduced to 50 g at which the penetration phase was started (Fig. 3). Before actuation, sufficient time was allowed to assure pore-pressure dissipation.

Table 3
Summary of the main test conditions

Soil	Sample	Test	Diameter (mm)	Length (mm)	Velocity (mm/s)
Kaolin-Sand	4	4S1	7	28	0.3
Kaolin-Sand	4	M1	14	56	0.2
Kaolin-Sand	4	B1	21	84	0.1
Kaolin-Sand	4	S2	7	28	0.3
Kaolin-Sand	4	M2	14	56	0.2
Kaolin-Sand	4	B2	21	84	0.1
Kaolin-Sand	5	S1	7	28	0.3
Kaolin-Sand	5	M1	14	56	0.2
Kaolin-Sand	5	B1	21	84	0.1
Kaolin-Sand	5	S2	7	28	0.3
Kaolin-Sand	5	M2	14	56	0.2
Kaolin-Sand	5	B2	21	84	0.1
Kaolin-Sand	6	S1	7	28	0.3
Kaolin-Sand	6	M1	14	56	0.2
Kaolin-Sand	6	B1	21	84	0.1
Kaolin-Sand	6	S2	7	28	0.3
Kaolin-Sand	6	M2	14	56	0.2
Kaolin-Sand	6	B2	21	84	0.1
Roncador	9	S1	7	28	0.3
Roncador	9	M1	14	56	0.2
Roncador	9	B1	21	84	0.1
Roncador	9	S2	7	28	0.3
Roncador	9	M2	14	56	0.2
Roncador	9	B2	21	84	0.1
Roncador	10	S1	7	28	0.3
Roncador	10	M1	14	56	0.2
Roncador	10	B1	21	84	0.1
Roncador	10	S2	7	28	0.3
Roncador	10	M2	14	56	0.2
Roncador	10	B2	21	84	0.1

The final thickness of the samples was typically 100 mm, corresponding to a depth of 5.00 m at prototype scale. This thickness allowed penetration tests to be carried out at a maximum depth of 60 mm (around 3.0 m).

Figure 4 shows the final water content profile for all samples. Almost identical profiles can be observed for samples 4, 5 and 6 (kaolin-sand mixture), and slight difference in the profiles for samples 9 and 10 (Roncador clay). The kaolin-sand clay samples (4, 5 and 6) presented an almost constant final water content value around 35%. Roncador clay samples (9 and 10) showed a linear decreasing trend, with water content values varying between 80% and 60%.

7. Test results

Figure 5 presents the six undrained shear strength profiles for all five samples. Although the strength ratios of extraction to insertion seem to be lower than expected (<0.6), the industrial load cell used in the tests performed efficiently and the data were considered reliable.

The presumed behaviour at shallow depths was that the smaller T-bar tests (S1 and S2) would show higher S_u values than those of the medium T-bar (M1 and M2). Additionally, the medium T-bar tests should show higher values than the larger T-bars.

However, this behaviour is only discernible in samples 5, 6 and 9, while in sample 10 all the profiles are very close to each other. Sample 4 shows better performance when considering only test S2, however the test S1 profile is very close to the medium and larger T-bar tests.

Fig. 3. Image of the penetration phase.
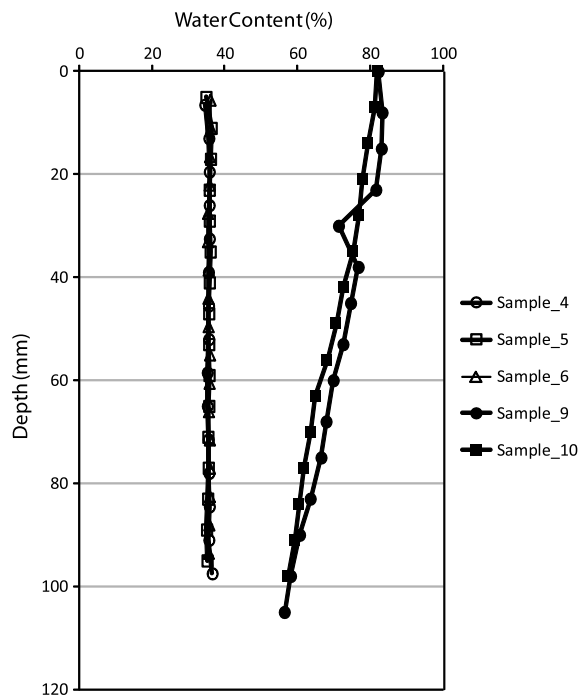
Fig. 4. Water content profile for all tests.
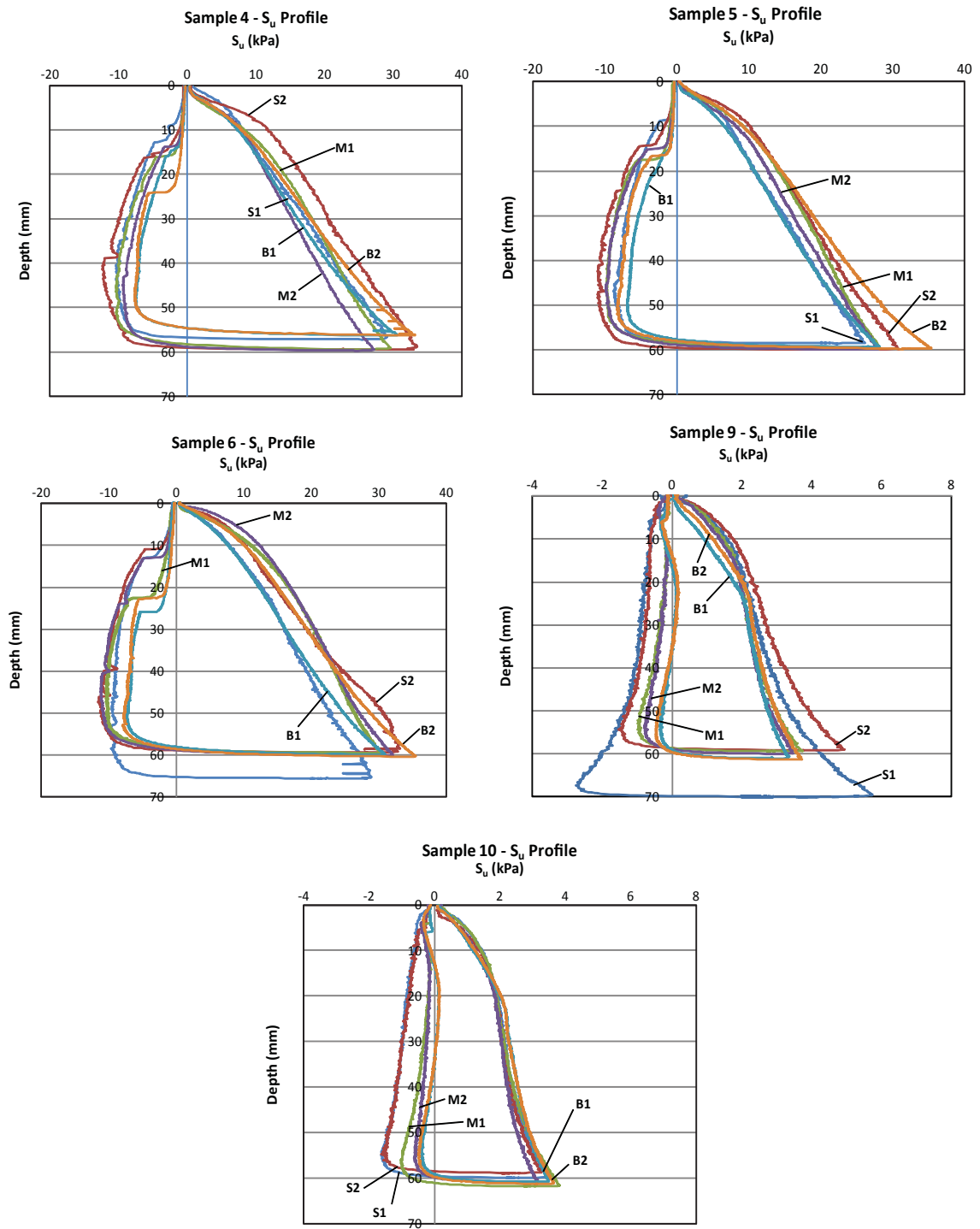
Fig. 5. Undrained shear strength profiles for all tests.

Table 4
Tests used to obtain the T-bar bearing factors

Soil	Sample	Smaller T-bar test	Larger T-bar test
Kaolin-Sand	4	S1	B1
Kaolin-Sand	4	S2	B2
Kaolin-Sand	4	M1	B1
Kaolin-Sand	5	S1	B1
Kaolin-Sand	5	S2	B1
Kaolin-Sand	5	S2	B2
Kaolin-Sand	5	S2	M1
Kaolin-Sand	5	M1	B1
Kaolin-Sand	6	S2	B1
Kaolin-Sand	6	M1	B1
Kaolin-Sand	6	M2	B2
Roncador	9	S1	B1
Roncador	9	S2	B1
Roncador	9	S2	M1
Roncador	9	S1	M2
Roncador	9	M1	B1
Roncador	9	M2	B2
Roncador	10	S1	B2
Roncador	10	S2	B1
Roncador	10	S1	M2
Roncador	10	S2	M1
Roncador	10	M1	B1

The expected behaviour of the strength profiles at greater depths is that the results will be very close to each other, showing that the measured undrained strength is the same regardless of the size of the T-bar tool. Though, this behaviour is not very clear in samples 4 and 6, in samples 5, 9 and 10 the profiles are essentially closer.

Based on the test concept described previously, where the comparison between the profiles from the smaller and larger T-bars can be used to assess the N_b factors at shallow depths, each test allows 12 different comparisons between the strength profiles obtained by the T-bar penetration tests (S1M1, S1M2, S2M1, S2M2, S1B1, S1B2, S2B1, S2B2, M1B1, M1B2, M2B1 and M2B2). However, only 6 or 7 comparisons were considered in order to contemplate issues such as site proximity between the tests and their relative position in the centrifuge box. This procedure was employed to avoid comparison between the strength profiles undertaken in the middle of the box and those obtained close to the strongbox edges. Table 4 shows the tests used to obtain the T-bar bearing factors.

8. Discussion of the results

Figure 6 presents the results of the selected comparisons between the smaller and larger T-bar profiles for all samples. A mean value curve is also provided for each sample along with the function proposed by [14] as a reference.

Kaolin-sand samples 4 and 5 showed similar behaviour with a mean $N_b \approx 9$ for $H/D = 100\%$ and $N_b \approx 10.5$ for $H/D = 300\%$, while sample 6 showed N_b between 8 and 10.5 for the same H/D interval.

Roncador sample 9 presented a mean $N_b \approx 7$ for $H/D = 75\%$ and $N_b \approx 9.5$ for $H/D = 175\%$, while sample 10 presented a flat distribution with N_b values varying between 9.5 and 10.5 for $75\% < H/D < 400\%$. Sample 10's atypical behaviour might be related to those reasons already mentioned in the previous section.

In general, all experimental data are above the numerical reference curve proposed by [14]. This result may be explained by the fact that the numerical curve is based on a homogeneous strength profile while the clay samples have an increasing strength with depth.

Figure 7 shows the consolidation of the mean value curves of samples 4, 5, 6 and 9 in comparison with the equations proposed by [14] and [13], considering that the first is based on a homogeneous strength profile and the
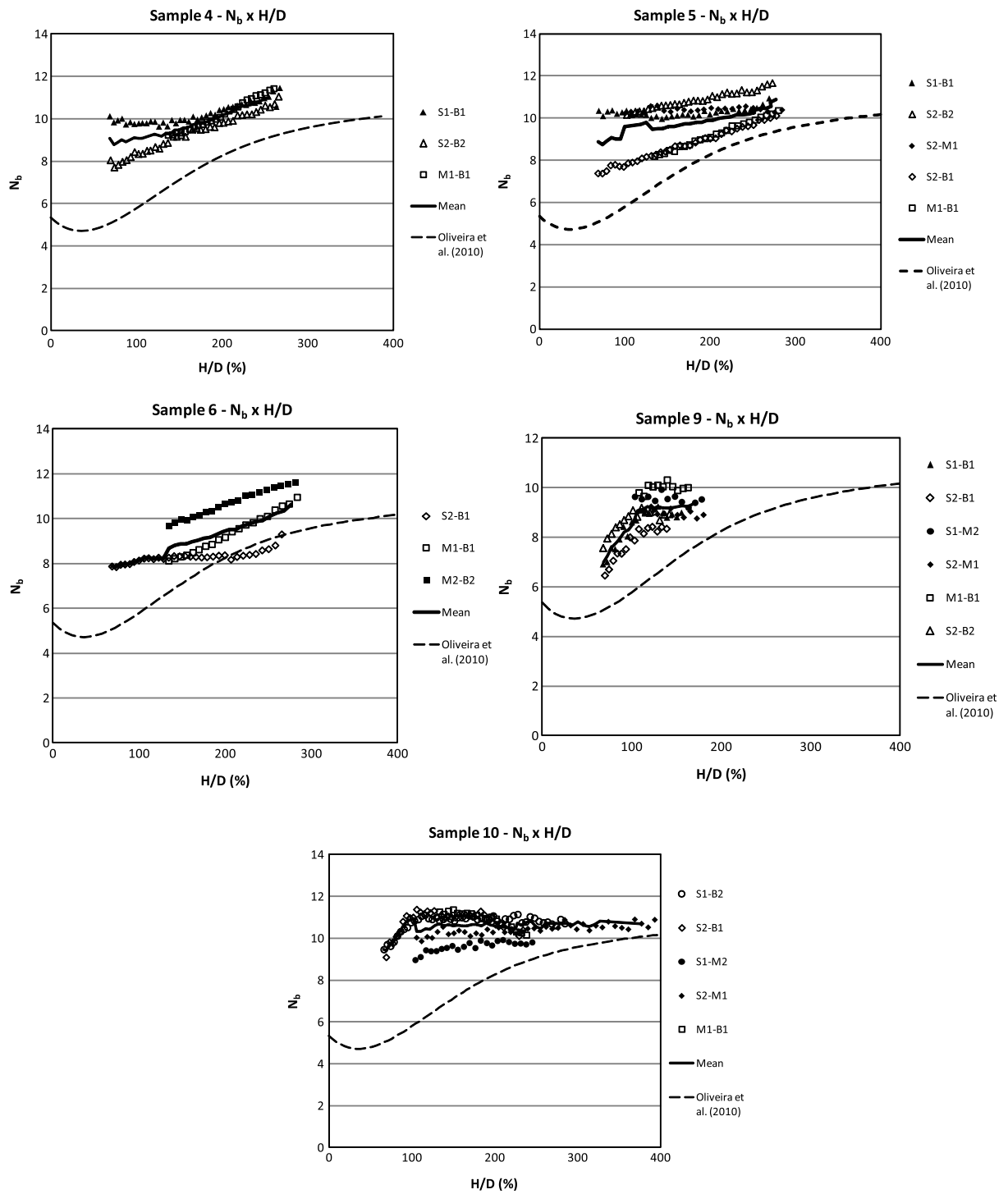
Fig. 6. T-bar factor (N_b) variation for all tests.
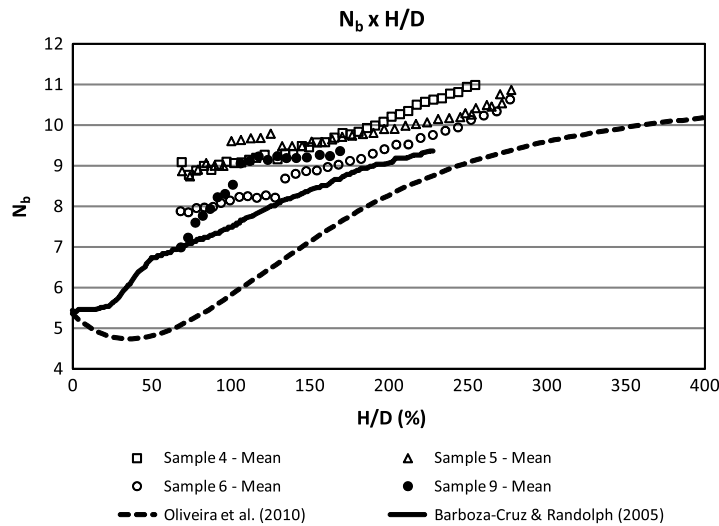
Fig. 7. Comparison between test results and literature.

Table 5
Comparison between experimental and Barboza-Cruz and Randolph (2005) data

Description	$H/D = 75\%$	$H/D = 100\%$	$H/D = 150\%$	$H/D = 200\%$
Kaolin-Sand sample 4	8.8	9.1	9.5	10.1
Kaolin-Sand sample 5	8.7	9.6	9.6	9.9
Kaolin-Sand sample 6	7.9	8.2	8.9	9.4
Roncador sample 9	7.2	8.5	9.2	–
Mean value for clay samples	8.2	8.9	9.3	9.8
Barboza-Cruz and Randolph (2005)	7.1	7.5	8.4	9.1
Variation (%)	15%	18%	11%	8%

second is based on a non-homogeneous strength profile. Sample 10 was discarded due to its atypical behaviour shown in Fig. 6.

As expected, [13] curve is closer to the experimental data than that of [14], since the clay samples' strength profiles are not as homogeneous as the former. Table 5 summarises the comparison between the clay samples' data and the numerical non-homogeneous curve. The calculated variation is between a minimum of 8% ($H/D = 100\%$) and a maximum of 18% ($H/D = 200\%$), with experimental data values always greater than the numerical ones.

9. Conclusions

A series of 30 centrifuge T-bar penetrometer tests were undertaken using three different bar sizes. In order to assess the T-bar bearing factor (N_b), the undrained strength profiles obtained from the small T-bar were compared with those profiles obtained for the larger ones. Generally, the experimental data presented higher N_b values than those predicted by [14] or [13] for all H/D ratios, although they were closer to the later which adopted a non-homogenous strength profile.

The calculated variation between the test results and the [13] equation is between a minimum of 8% ($H/D = 100\%$) and a maximum of 18% ($H/D = 200\%$).

Acknowledgments

References

[1] Chung SF, Randolph MF. Penetration resistance in soft clay for different shaped penetrometers. Proc 2nd Int Conf on Site Characterisation, Porto, 2004;pp. 671-677.

[2] Randolph MF. Offshore Geotechnics –the challenges of Deepwater Soft Sediments. In: Geotechinical Engineering State of the Art and Practice. GeoCongress 2012. ASCE Geotechinical Special Publication No. 226.

[3] Lunne T, Andersen K, Low HE, Sjursen M, Li X, Randolph MF. Guidelines for offshore *in situ* testing and interpretation in deep water soft soils. Canadian Geotech J 2011;48(6):543-556.

[4] Stewart DP, Randolph MF. T-bar penetration testing in soft clay. J of Geotech Eng Div, ASCE 1994;120(12):2230-2235.

[5] Oliveira JRMS, Almeida MSS. Pore-pressure generation in cyclic T-bar tests on clayey soil. In: International Journal of Physical Modelling in Geotechnics 2010;10:19-24.

[6] Stewart DP, Randolph MF. A new site investigation tool for the centrifuge, *Proc Int Conf on Centrifuge Modeling –Centrifuge '91*, Boulder, Colorado, 1991; 531-538.

[7] Watson PG, Newson TA, Randolph MF. Strength profiling in soft offshore soils, Proc 1st Int Conf on Site Characterisation - ISC '98, Atlanta, 1998;21389-1394.

[8] Almeida MSS, Oliveira JRMS, Motta HPG, Almeida MCF, Borges RG. CPT and T-bar Penetrometers for Site Investigation in Centrifuge Tests. Soils and Rocks, São Paulo 2011;34(1):79-88.

[9] Randolph MF, Houlsby GT. The limiting pressure on a circular pile loaded laterally in cohesive soil, Geotechnique 1984;34(4):613-623.

[10] Randolph MF. Characterization of soft sediments for offshore applications. Proc Geotechnical and Geophysical Site Characterization, Millpress, Rotterdam, 2004; pp. 209-232.

[11] Low HE, Lunne T, Anderesen KH, Sjursen MA, Li X, Randolph MF. Estimation of intact and remoulded undrained shear strength frompenetration tests in soft clays. Géotechnique 2010;60(11):843-859.

[12] Low HE, Randolph MF, Lunne T, Anderesen KH, Sjursen MA. Effects of soil characteristics on relative values of piezocone, T-bar and ball penetration resistances. Géotechnique 2011;61(8):651-664.

[13] Barboza-Cruz ER, Randolph MF. Bearing capacity and large penetration of a cylindrical object at shallow embedment. Proc Frontiers in offshore geotechnics, Australia: Perth, 2005. pp. 615-621.

[14] Oliveira JRMS, Almeida MSS, Almeida MCF, Borges RG. Physical Modeling of Lateral Clay-Pipe Interaction. Journal of Geotechnical and Geoenvironmental Engineering 2010;136:950-956.

[15] White DJ, Gaudin C, Boylan N, Zhou, H. Interpretation of T-bar penetrometer tests at shallow embedment and in very soft soils. Canadian Geotechnical Journal 2010;47(2):218-229.

[16] Oliveira JRMS, Almeida MSS, Motta HPG, Almeida MCF. Influence of penetration rate on penetrometer resistance. Journal of Geotechnical and Geoenvironmental Engineering 2011;137:695-703.

[17] Neto JLS, Oliveira JRMS, Almeida MSS, Almeida MCF, Fagundes DF. Retrofits to COPPE mini-drum geotechnical centrifuge. Proc 7th Int Conf on Physical Modelling in Geotechnics, Zurich, 2010;1:211-216.

[18] Fagundes DF, Rammah KI, Almeida MSS, Pequeno J, Oliveira JRMS, Borges RG. Strength Behaviour Analysis of an offshore Brazilian Marine Clay. Proc 31st Int Conf on Ocean, Offshore and Artic Engineering, 2012.

[19] Chung SF, Randolph MF, Schneider JA. Effect of penetration rate on penetrometer resistance in clay. Journal of Geotechnical and Geoenvironmental Engineering, ASCE, 2006;132(9):1188-1196.